



Abstract

The derivation of the coronal proton bulk speed is one of the main goals of the Metis coronagraph on board the Solar Orbiter S/C. Metis is capable of acquiring both visible-light (VL) broadband (580-640 nm) polarized brightness (pB) images and ultraviolet (UV) HI Lyman-alpha (121.6 nm) images simultaneously with high temporal (up to 1 s for the UV and 60 s for VL/pB) and spatial (down to 4500 km/pixel) resolution. The proton outflow speed is derived from these data through the Doppler-dimming diagnostics. Here solar wind speed maps are presented that are derived for three Solar Orbiter Remote Sensing Windows. This outlines the evolution of the solar wind during half of the 25th solar cycle (from the end 2021 to the end 2023). Different literature electron temperature profiles are used as a parametric input for the Doppler-dimming diagnostics, thus deriving the sensitivity of the Doppler-dimming diagnostics to the knowledge of the electron temperature profile of the coronal plasma in different regions in the field of view (e.g. streamer, coronal holes). Preliminary results show the role played by the knowledge of the coronal electron temperature in the derivation of the solar wind maps.

Data Analysis

Our data set consist of Metis [1] VL-pB and UV Ly α data representative of three distinctive periods of the current solar cycle no. 25:

1. near the solar minimum (2021-09-21)
2. during the ascending phase (2022-10-13)
3. approaching to the maximum (2023-04-09)

The VL-pB and UV intensities are given by

$$pB \propto \int_{LoS} n_e(x) dx$$

$$I_{Ly\alpha} \propto \int_{LoS} R(T_e) n_e(x) \Phi(v_w, T_k, I_{\odot}) dx$$

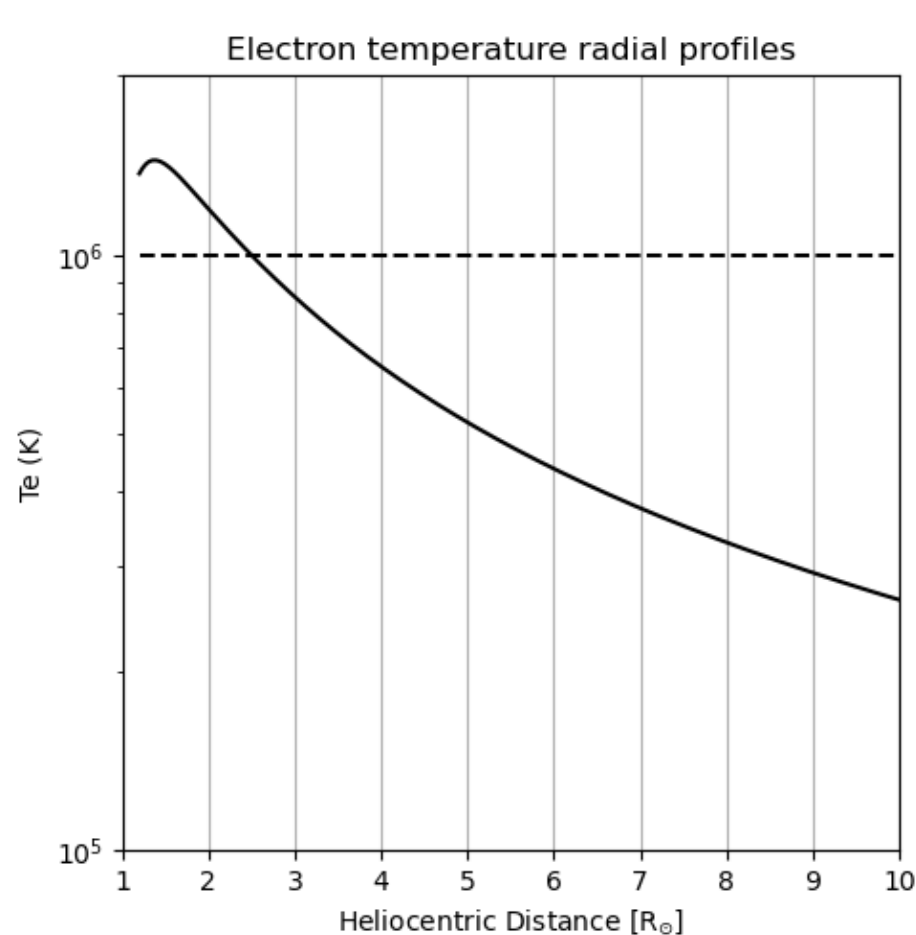
and depend upon several physical and geometrical parameters: the electron number density n_e ; the hydrogen ionisation ratio R , which depends upon the electron temperature T_e ; the Φ factor represents the UV doppler dimming due to the presence of coronal outflow speed v_w , the kinetic temperature of the scattering ions T_k and the exciting chromospheric radiation I_{\odot} [2],[3],[4],[5]. From the acquired pB images it is possible to derive the electron density profiles in the plane of the sky (PoS) using the standard van de Hulst inversion technique [3].

We made use of the Doppler Dimming Tool (DDT; Giordano S. et al., in prep.) to derive the solar-wind outflow speed. The DDT assumes an axisymmetric distribution of the electron density w.r.t. the solar rotational axis, and it takes as input all the other physical and geometrical parameters described above, giving as output the SW outflow speed derived through the Doppler-dimming inversion method.

Here we derived the SW speed maps considering two different assumptions for the electron temperature:

- a uniform temperature of 10^6 K all over the image field of view;
- a varying temperature given by the radial profile derived for an equatorial streamer at solar minimum by Gibson+[6] (Fig. 1)

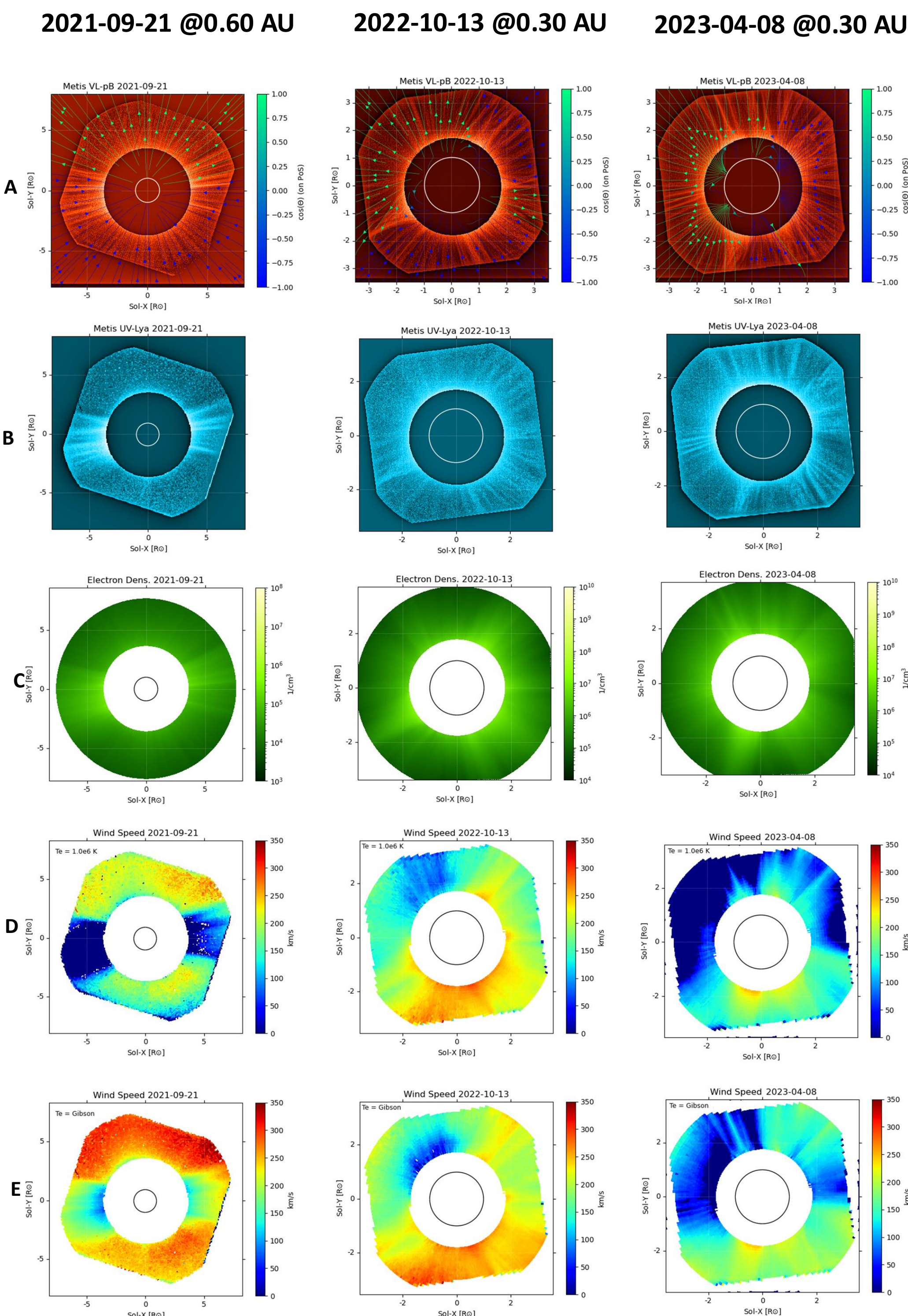
Fig.1 A varying radial electron temperature profile, following that of Gibson+[6] (thick line); and a 1.0^6 K uniform radial temperature profile (dashed line).



The input data sets and the corresponding Doppler-dimming derived SW speed maps are shown in Fig.2. The Multi-scale-Gaussian-Normalising filter [7] is used here only to enhance the coronal structures and to over plot the magnetic field lines extrapolated by the Wave-Turbulence-Driven PSI-MAS model [8].

Maps of the Solar Wind Speed derived from the VL-pB & UV-Lya Metis Images

Fig. 2 Row A: VL-pB (filtered using the MGN filter), PSI-MAS magnetic field lines are over-plotted; Row B: UV-Lya (filtered as in A); Row C: Electron Densities (cm^{-3}), derived from the VL-pB; Row D: Solar Wind Speed maps (km/s) assuming a uniform $Te=10^6$ K along the LoS; Row E: Solar Wind Speed maps (km/s) assuming a varying Gibson profile along the LoS. Rows C,D,E are all derived with the DDT.



Results

- Metis provides for the first time global maps of the solar wind outflow speed in the inner corona on a regular basis throughout the Solar Orbiter mission.
- The varying radial electron temperature assumption seems to be a more suitable input hypothesis to the DDT, since the solar minimum phase Doppler-dimmed derived SW speed map has values that are more physically reasonable w.r.t. the uniform 10^6 K assumption, in these heliocentric distances
- On the other hand, during the rising and near-maximum phases slow and fast coronal regions are more intermingled. In this case, the uniform temperature assumption may represent a LoS average of a radially varying electron temperature profile. This may not be the case in the more defined slow/fast regions near-maximum, where gradient of electron temperature along the LoS gives a better distribution of the neutral hydrogen abundance.
- The qualitative comparison between the WTD PSI-MAS field-lines geometry and the MGN filtered VL-pB images shows an overall agreement w.r.t. the topology of streamer/coronal hole regions.

The electron temperature distribution in the solar corona represents an important input parameter in the derivation of the outflow velocity through the Doppler-dimming technique, and different assumptions lead to different determinations of the solar wind speed.

Future directions

- Deriving the outflow velocity by assuming different electron temperature profiles along the LoS (e.g. [9]) and different models, taking into account the radial variation of the electron temperature [10].
- The NASA-KASI-INAF Coronal Diagnostic Experiment (CODEX) [11] launch to ISS is scheduled on Sept 2024. CODEX is equipped with five narrowed pass-band filters (centered 3900 Å, 4103 Å, 3987 Å, 4233 Å) and a broadband filter (3800 – 4300 Å). Its observations will be used to simultaneously derive the solar wind speed, the electron density and the electron temperature in a 3 – 8 Rsun FoV, thus completing also the Metis data and better constraining the coronal models.

References

[1] Fineschi et al. 2020, Geophys. Res., **104**, Exp. Astron., **49**, 239
 [2] Antonucci E., et al. 2020, A&A **642**, A10
 [3] van de Hulst, H. C. 1950, Bull. Astron. Inst. Neth., **11**, 135
 [4] Noci, G., Kohl, J. L., & Withbroe, G. L. 1987, ApJ, **315**, 706
 [5] Withbroe, G. L. et al., 1982, Space Sci. Rev., **33**, 17
 [6] Gibson et al., 1999
 [7] Morgan, H., & Druckmüller M., Sol. Phys., **289**, 2945
 [8] Mikić, Z., et al. 2018, Nat. Astr., **2**, 913
 [9] Vázquez, A. M. et al 2003 ApJ, **598** 1361
 [10] Lemaire, J.F., & Stegen, K., 2016, Sol Phys, **291**, 3659
 [11] Newmark, J., et al., 2020, NASA tech-report